

**High-Throughput Well Plate Approach Illustrates Strain Specific
Variation in Picocyanobacteria Nitrogen and Phosphorus Usage**

By

Tanner P. Cormier

A thesis submitted to the

Department of Biology

Mount Allison University

in partial fulfillment of the requirements for the
Bachelor of Science degree with Honours in Biology

April 11, 2022

Table of Contents

TABLE OF CONTENTS	I
TABLE OF FIGURES AND TABLES	II
ACKNOWLEDGEMENTS	IV
ABSTRACT	1
INTRODUCTION	2
Picrocyanobacteria and their significance	2
Climate Change and Environmental Relevance	3
Strain Specifications	6
Niche Study and Determination	6
Study Aims	7
METHODS	8
Culturing and Media protocols	8
Experimental protocol	11
Inoculation Culture Preparation	12
Controlled Culturing	13
Data Collection	15
Data Analysis	15
Importing Data	15
Data Modeling and Analyses	16
Model for Between Strain Comparisons	16
Model for Within-Strain Comparisons	17
RESULTS	18
Identifying nutrient-dependent maximum growth duration and culture densities	18
Between Strain Nutrient Comparison	19
Within-Strain Nutrient Comparison	20
CZS25K	21
CZS48M	25
PCC6803	28
DISCUSSION	31
General Findings	31
Relevance of Findings	32
REFERENCES	38
APPENDIX	44

Table of Figures and Tables

TABLE 1: COMPONENTS ADDED TO SIX LITRES OF MILLI-Q FOR SALT SOLUTION I PRODUCTION OF ARTIFICIAL SEAWATER DEVELOPED BY (HARRISON ET AL., 1980) AND MODIFIED BY (BERGES ET AL., 2001).

9

TABLE 2: COMPONENTS ADDED TO THREE LITRES OF MILLI-Q FOR SALT SOLUTION II PRODUCTION OF ARTIFICIAL SEAWATER DEVELOPED BY (HARRISON ET AL., 1980) AND MODIFIED BY (BERGES ET AL., 2001).

10

TABLE 3: BG11 MEDIA STOCKS (ADDED TO ARTIFICIAL SEAWATER TO PRODUCE MEDIA) DEVELOPED BY (ALLEN AND STANIER, 1968) AND MODIFIED BY (WATANABE ET AL., 2000). THE NUTRIENT STOCKS WERE PREPARED BY ALYSON MACCORMACK AND STORED IN A STANDARD LABORATORY REFRIGERATOR TO MINIMIZE DETERIORATION.

10

TABLE 4: BG11 TRACE METAL STOCK SOLUTION PROTOCOL DEVELOPED BY (ALLEN AND STANIER, 1968) AND MODIFIED BY (WATANABE ET AL., 2000). THE SOLUTION WAS PREPARED BY ALYSON MACCORMACK AND STORED IN A STANDARD LABORATORY REFRIGERATOR TO MINIMIZE DETERIORATION.

11

FIGURE 1: EXPERIMENTAL WORKFLOW SCHEMATIC.

11

FIGURE 2: WELL MEDIA CONCENTRATIONS USED FOR CONTROLLED CULTURING EXPERIMENTAL EXAMINATION. EACH PLATE CONTAINED TWO SEPARATE PICOCYANOBACTERIA STRAINS DURING TRIALS. ONE STRAIN WOULD BE CONTAINED IN COLUMNS 1 TO 4, AND THE SECOND STRAIN, WITH A DIFFERENT MEDIA SALINITY, WAS GROWN IN COLUMNS 5 TO 8. FINAL NITRATE CONCENTRATION IS REPRESENTED BY POINT SIZE, AND FINAL PHOSPHATE CORRESPONDS TO POINT COLOUR. THE NUTRIENT MATRICES ARE DUPLICATES FOR EACH STRAIN

14

FIGURE 3: METRICS OF MAXIMUM GROWTH DURATION (CELL COUNT) AND DURATION (DAYS) CREATED USING ROLLING CHANGES IN CELL COUNTS FROM DAILY MEASUREMENTS. NITRATE CONCENTRATION (μM) IS REPRESENTED BY DATA POINT SIZE, AND PHOSPHATE CONCENTRATION (μM) IS A CONTINUOUS NUMERIC COLOUR GRADIENT.

19

FIGURE 4: NON-METRIC MULTI-DIMENSIONAL SCALING (NMDS) CREATED WITH A BRAY CURTIS DISTRIBUTION TO REPRESENT STRAIN GROWTH RATES MODELLED BY A MODIFIED GOMPERTZ EQUATION, USED TO MODEL BETWEEN STRAIN VARIATION BASED ON NUTRIENT CONCENTRATION. NITRATE CONCENTRATION (μM) IS REPRESENTED BY DATA POINT SIZE, AND PHOSPHATE CONCENTRATION (μM) IS A CONTINUOUS NUMERIC COLOUR GRADIENT.

20

FIGURE 5: BOXPLOT REPRESENTATION OF CZS25K GROWTH RATES PRODUCED USING THE MODIFIED GOMPERTZ EQUATION TO CREATE A GROWTH RATE METRIC USING CELL COUNTS COLLECTED TO MONITOR CULTURE-SPECIFIC GROWTH. THE DATA IS DIVIDED BY NITRATE CONCENTRATION AND ORGANIZED FOR SIDE-BY-SIDE PHOSPHORUS COMPARISONS WITHIN EACH LEVEL OF NO_3 .

22

TABLE 5: POST HOC COMPARISON CREATED USING AN ARTOOL ALIGNED RANKED TRANSFORM CONTRASTS (ART.CON) APPROACH. ONE FACTOR AND INTERACTION NUTRIENT COMPARISONS ORGANIZED BY COLUMN ARE REPRESENTED FOR CZS25K.

22

FIGURE 6: BOXPLOT REPRESENTATION OF CZS48M GROWTH RATES PRODUCED USING THE MODIFIED GOMPERTZ EQUATION TO CREATE A GROWTH RATE METRIC USING CELL COUNTS COLLECTED TO MONITOR CULTURE-SPECIFIC GROWTH. THE DATA IS DIVIDED BY NITRATE CONCENTRATION AND ORGANIZED FOR SIDE-BY-SIDE PHOSPHORUS COMPARISONS WITHIN EACH LEVEL OF NO_3 .

26

TABLE 6: POST HOC COMPARISON CREATED USING AN ARTOOL ALIGNED RANKED TRANSFORM CONTRASTS (ART.CON) APPROACH. ONE FACTOR AND INTERACTION NUTRIENT COMPARISONS ORGANIZED BY COLUMN ARE REPRESENTED FOR CZS48M. _____27

FIGURE 7: BOXPLOT REPRESENTATION OF PCC6803 GROWTH RATES PRODUCED USING THE MODIFIED GOMPertz EQUATION TO CREATE A GROWTH RATE METRIC USING CELL COUNTS COLLECTED TO MONITOR CULTURE-SPECIFIC GROWTH. THE DATA IS DIVIDED BY NITRATE CONCENTRATION AND ORGANIZED FOR SIDE-BY-SIDE PHOSPHORUS COMPARISONS WITHIN EACH LEVEL OF NO_3 .29

TABLE 7: POST HOC COMPARISON FOR PCC6803. IT WAS CREATED USING AN ARTOOL ALIGNED RANKED TRANSFORM CONTRASTS (ART.CON) APPROACH. THERE ARE REPRESENTATIONS OF ONE-FACTOR NUTRIENT COMPARISONS WITH THE ABSENCE OF AN INTERACTION, ORGANIZED INTO COLUMNS BASED ON NUTRIENT TYPE (NITRATE OR PHOSPHATE). _____29

Acknowledgements

A huge thank you goes out to everyone that has helped or supported me through the process of completing my thesis. First of all, my supervisors, Dr. M Berthold and Dr. DA Campbell. Dr. Berthold, thank you for all the guidance and wisdom you have given me and your kindness and patience during the many obstacles I have faced throughout the year. Dr. Campbell, thank you for giving me the initial push I needed to pursue this project and for your continued support throughout its completion. Special thanks also go out to Naaman Omar and Mireille Savoie for creating a welcoming lab environment and always being willing to lend a hand or answer questions. Also, to Yahya Farooqi for his support and camaraderie as we embarked on this journey together. Thank you to the NB Tel Fund, the FundyPhytoPhys Lab, and Mount Allison University for providing the funding necessary for completing my research. And finally, Dr. J Liefer for his help and advice as my committee member and second reader.

I would also like to thank the many friends and family who have offered me tremendous support throughout my many academic endeavours. To my mother, Jeannie Cormier, father, Paul Cormier, and Aunt Rosemary Stark for always being willing to pick up the call and offer words of advice or encouragement when I needed it most. Finally, Erin MacMillan, Lindsey Partington, Mackenzie Scott, SunMin Park and Jamee MacNeil for being a major part of my honours and final year at Mount Allison.

Abstract

In the wake of water body eutrophication influenced by major nutrient influxes from agriculture and urban runoff, there have been global increases in the growth of phytoplankton species. The environments created appear to favour the growth of cyanobacteria in comparison to other primary producers. The smallest group of these organisms, known as picocyanobacteria, is uniquely adapted to grow and dominate aquatic environments following a period of nutrients saturation. Due to the small nature of these organisms' identification outside of genomic testing can be a difficult task, as such minor morphological differences can be hard to identify using microscopic techniques. Despite being closely related and similarly classified, many picocyanobacteria have been highly specialized in their environment based on conditions such as salinity, nutrient availability, and light. This study implemented the use of a high-throughput well plate design to expose three strains of picocyanobacteria to a fully crossed experimental matrix of five phosphorus concentrations (0 μM , 0.5 μM , 3.0 μM , 5.0 μM , and 7.0 μM), four nitrogen concentrations (0 μM , 5.0 μM , 30.0 μM , and 70.0 μM), and three-light levels (30, 100 or 300 $\mu\text{mol photons m}^{-2} \text{ s}^{-1}$), to determine if niche determination based on nutrients and light is an effective method of understanding and characterizing the growth of picocyanobacteria strains. *Cyanobium* sp. CZS25K, *Cyanobium* sp. CZS48M, and *Synechocystis* sp. PCC6803 were examined for this study. Statistical modelling demonstrated distinct strain-specific variations between the uses of nutrients and light for growth. Nitrogen and phosphorus concentrations were demonstrated to influence the growth of CZS25K. Nitrogen and light levels were essential for the growth of CZS48M. In contrast, PCC6803 growth rates were most sensitive to environmental nitrogen availability. These results may help support and inspire studies examining phytoplankton growth and adaptation mechanisms. This knowledge is becoming increasingly valuable for global monitoring and management of accelerated phytoplankton growth.

Introduction

Picocyanobacteria and their significance

Picocyanobacteria form one of the smallest groups of cyanoprokaryotes, typically measuring less than 3 μm in diameter (Jasser and Callieri, 2016). There are four main groups used for their classification: *Synechococcus*, *Prochlorococcus*, *Cyanobium*, and *Synechocystis* (Komárek, 2010; Lopes et al., 2012). Overall, picocyanobacteria have a broad distribution, but distinctions can be made on a strain-specific basis. Globally *Synechococcus* can be found within marine and fresh waters (Kim et al., 2018), *Prochlorococcus* inhabits marine environments (Thompson et al., 2018), *Cyanobium* occupy brackish and fresh waters (Albrecht et al., 2017). Meanwhile, *Synechocystis* only maintain the ability to grow in freshwater (Jasser and Callieri, 2016). Picocyanobacteria can adapt to their environment, and modern research demonstrates that climate change influences seem beneficial to picophytoplankton compared to their larger counterparts (Schmidt et al., 2020).

The characteristic that provides the most significant advantage to picocyanobacteria is their size. Cell size is vital for most functions within photosynthetic microbes. This idea gives rise to the package effect, which infers that larger cells are less effective at photosynthesizing than their smaller counterparts based on differences in pigment absorption compared to their potential (Malerba et al., 2018). Several assumptions define this. To begin, there is an increase in diffusion-regulated nutrient uptake due to smaller cell sizes and thinner cell membranes (Raven, 1998). In addition to nutrient uptake advantages, small cell size and packing effect allows picophytoplankton to require a much smaller nutrient flux for survival and growth (Raven, 1998). More recent

findings suggest that photosynthetic capacity is likely controlled by trade-offs between chlorophyll and volume-specific determinants within a cell (Malerba et al., 2018). Even though their examination only recently became a major research field, picocyanobacteria compose over 50% of the cyanobacterial biomass found worldwide and are essential to the carbon cycle as they can contribute as much as 5% to 90% of all aquatic carbon depending on trophic level (Stockner, 1988; Flombaum et al., 2013). Despite this, the recent increase of picophytoplankton production has shown to be detrimental to aquatic food webs. Species such as fish, seabirds and marine mammals rely on phytoplankton consumers like mesozooplankton as major contributors to their dietary needs (Kiørboe, 2018). As picophytoplankton shift to controlling larger portions of primary producer abundance, they cannot function as a nutritional substitute. Unlike organisms such as diatoms, picocyanobacteria have limited nutrient stores and do not produce biomolecules such as omega-3 polyunsaturated fatty acids and sterols, which are essential to organisms in higher trophic levels (Jónasdóttir, 2019; Ruess and Müller-Navarra, 2019; Schmidt et al., 2020). In addition, there is a minimal connection between picocyanobacteria and the higher food chain as they are too small to be consumed by organisms such as copepods (Kiørboe, 2018).

Climate Change and Environmental Relevance

As global populations rise, there has been a simultaneous intensification of agricultural practices, which have made significant contributions to nutrient pollution of water bodies (Tilman, 1999). In the 34 years before 1999, nitrogen fertilization achieved a 6.87-fold increase, and phosphorus fertilization faced a 3.48-fold increase (Tilman, 1999). Commonly, the amount of fertilizer applied to crops and the amount used by these plants

is much higher than what is required leaving the excess to be washed away (Liu et al., 2008). Nutrient runoff into both fresh and marine water bodies has produced significant saturation of nutrients such as nitrogen and phosphorus, known as eutrophication (Tilman, 1999). Most fertilizers are composed of nitrogen, phosphorus, and potassium ratios, which account for the high nitrate and phosphate levels within agricultural run-off. In addition, urban runoff also contributes major contributions to water body eutrophication. There are three main ways nitrogen and phosphorus accumulate in urban waste products. The first is nutrient deposition from the atmosphere (Kaushal et al., 2011; Hobbie et al., 2017; Yang and Lusk, 2018). Secondly, anthropogenic sources that originate from human activities (Yang and Lusk, 2018). Anthropogenic sources include the use of chemicals (fertilizers, for example), human fecal and urine waste, as well as many other mechanisms by which pollutants are introduced to the environment (Anisfeld et al., 2007; Kaushal et al., 2011; Mueller et al., 2016; Yi et al., 2017; Yang and Lusk, 2018). Finally, there are biogenic sources, such as those from the decay of organic matter (Hobbie et al., 2013; Duan et al., 2014; Yang and Lusk, 2018). One of the main consequences of eutrophication of water bodies, with urban and agricultural origins, is harmful algal blooms of phytoplankton, including strains of picocyanobacteria (Stal et al., 2003). This is in part due to an increased abundance of environmental nutrients. Researchers generally understand that phytoplankton growth rates are influenced by temperature, light, and nutrient availability, particularly nitrogen and phosphorus (Berthold and Campbell, 2021). Initially, removing increased nutrient levels was thought to be a solution, but long-term monitoring in regions like the Baltic sea shows that once a population or community comes to dominate an environment, it becomes resistant to change (Pyhälä et al., 2014).

Modern research acknowledges that to predict phytoplankton growth, the input and output of nutrients into the habitat are insufficient; multiple factors need to be examined, including temperature, illumination changes, and nutrient recycling (Berthold and Campbell, 2021). Because of their critical roles in eutrophication and picocyanobacteria growth, the paper will focus on examining the role of nitrate and phosphate on changes in growth rate.

There are two additional considerations that this study will attempt to account for, and they are environmental light gradients and initial culture density. As with all other photosynthetic organisms, phytoplankton require access to light, but aquatic environments create unique characteristics. Naturally, the light intensity will change based on depth in the water column (Lionard et al., 2005), but eutrophication-induced phytoplankton growth also influences environmental light availability. Many previous studies have evaluated the idea of culture self-shading using concepts like cell size (Agustí, 1991b). Self-shading acts as a mechanism of controlling culture density because as phytoplankton grow, they block light availability to the rest of their environment, weakening the photosynthetic abilities of other primary producers in their direct proximity (Agustí, 1991b). In terms of cell size, the larger the phytoplankton is, the more light they will block (Agustí, 1991b), but what are its applications to smaller-sized phytoplankton? As previously discussed, nutrient eutrophication has led to excessive algal growth within waterbodies due to a reduction in nutrient limitations (Schindler, 2006). This leads to the idea of culture density in terms of self-shading. Phytoplankton with larger cell sizes block light because of their greater biomass, but smaller cells in denser cultures may have a similar impact (Agustí, 1991b). Therefore, when nutrient levels do not restrict phytoplankton growth, a

decline in light intensity may limit maximum growth density (Agusti et al., 1990; Agustí, 1991b). The experimental design of this study includes three levels of light to account for any influence difference in light availability may have on picocyanobacterial growth. Additionally, from suggestions in previous studies, all initial cultures were cell counted and diluted to a density of about 500,000 cells/mL to minimize any influence from nutrient or light competition based on high initial culture density (MacCormack, 2021).

Strain Specifications

This study included the examination of three strains which are *Cyanobium* sp. CZS25K, *Cyanobium* sp. CZS48M, and *Synechocystis* sp. PCC6803. Experimentation on these strains allows for the development of a methodology that can be applied to further research on picocyanobacteria ecophysiology and niche determination. Based on the work of A. MacCormack & M. Berthold (unpub.), we know that CZS25K and CZS48M are suited for brackish salinity levels, and PCC6803 requires freshwater conditions. To substitute these varying requirements, the salinity of media used will be 11 and 1 ppt, while all other experimental variables will remain consistent across strains. This study attempted to determine the initial inoculation density of cultures so that the study could be more ecologically relevant and for the prevention of introducing unexpected variables such as increased nutrient competition or population density dependencies.

Niche Study and Determination

When working with microscopic organisms smaller than 3 μm , identification methods that deliver consistent and accurate results are limited. This can be especially important for situations like isolating and identifying the phytoplankton that composes an

algal bloom. Various novel microscopic techniques are being developed that show promise for this purpose, but this study aims to determine if nutrient niche determination can be used as a proxy for characterizing strains of picocyanobacteria in the meantime. Previous and co-current studies in our lab by A. MacCormack & M. Berthold (unpub.) and Y. Farooqi (unpub.) have focused on niche determination of these strains in terms of salinity and temperature. However, this research will focus on the specific roles of phosphorus and nitrogen concentrations in cyanobacterial growth. Fundamental niche determination examines the combination of abiotic factors and interactions between biotic and abiotic conditions that are most favourable for an organism within its environment (Hutchinson, 1957). With this information, it is also possible to define the conditions that are detrimental to the growth and survival of the focus strains.

Study Aims

This study aims to implement a high throughput, well-plate design to examine the physiological responses of *Cyanobium* sp. CZS25K, *Cyanobium* sp. CZS48M, and *Synechocystis* sp. PCC6803. Growth and acclimation patterns will be observed under phosphate and nitrogen depletion and repletion and across the experimental gradient of nutrient and light levels. Support for nutrient niche determination as an effective method of characterizing picocyanobacterial growth is gained when strain-specific growth patterns demonstrate significant variability based on environmental nitrate and phosphate abundance. Statistical analyses were used to detect distinct strain growth patterns based on experimental light and nutrient concentrations, determining strain-specific growth niches.

Methods

Culturing and Media protocols

For this project, BG11 media based on the protocols (contents represented in tables 3 and 4) developed by (Allen and Stanier, 1968) and modified by (Watanabe et al., 2000) found in (Andersen et al., 2005) were used for all culturing of, *Cyanobium* sp. CZS25K, *Cyanobium* sp. CZS48M, and *Synechocystis* sp. PCC6803. The strains used for experimentation are naturally found in brackish environments except for PCC6803 which prefers freshwater environments. To simulate this in the laboratory, BG11 media was produced using artificial seawater (ASW) (components of which are outlined in tables 1 and 2) according to the recipe produced by (Harrison et al., 1980) and modified by (Berges et al., 2001). The ASW used to produce the BG11 media was diluted with Milli-Q and autoclaved for sterilization based on the optimal media salinity for each strain determined by A. MacCormack & M. Berthold (unpub.). CZS25K and CZS48M were cultured in 11ppt media, and PCC6803 was grown in 1 ppt media. Once the ASW reached the desired salinity, filter-sterilized BG11 stocks (outlined in tables 3 and 4) were added to each of the media bottles, and autoclaved Milli-Q was added to ensure each bottle contained a litre of media to compensate for the volume lost in the autoclave. Next, a 20mL subsample of the media was pH corrected to 7.5 using 1M HCL and a Vernier pH probe. Once the volume of HCL needed to adjust the 20mL sample was determined, it was scaled to the volume remaining in the media bottle. Using filter-sterilized HCL, the scaled volume was added to the media bottle so that it could be adjusted as well.

This experiment required using both nitrogen and phosphorus replete and depleted media. Replete BG11 media was created following the typical procedure with N and P

stocks added as usual, and N and P-free media was made by withholding the NaNO_3 and K_2HPO_4 stocks during the production of the BG11 media.

The mother cultures were grown using a separate protocol from active experimental cultures. The test tubes of mother cultures were maintained using a 22°C incubator with a 12:12 light to dark photoperiod and $100 \mu\text{mol photons m}^{-2}\text{s}^{-1}$ of light. The mother culture tubes rack was placed on a shaker that rotated 120 times per minute. Every seven days, samples of the mother cultures would be transferred into new nitrogen and phosphorus replete BG11 media for culture maintenance. This process used 5 mL of the previous culture and 20 mL of fresh media added to each new culture. The experimental protocol section will explain the preparation of cultures through exposure to nitrogen and phosphorus depletion.

Table 1: Components added to six litres of Milli-Q for Salt Solution I production of artificial seawater developed by (Harrison et al., 1980) and modified by (Berges et al., 2001).

Components: Anhydrous salts	Quantity (g)	Molar concentration in the final medium
NaCl	211.940	3.63×10^{-1}
Na_2SO_4	35.500	2.50×10^{-2}
KCl	5.990	8.03×10^{-3}
NaHCO_3	1.740	2.07×10^{-3}
KBr	0.863	7.25×10^{-4}
H_3BO_3	0.230	3.72×10^{-4}
NaF	0.028	6.67×10^{-5}

Table 2: Components added to three litres of Milli-Q for Salt Solution II production of artificial seawater developed by (Harrison et al., 1980) and modified by (Berges et al., 2001).

Components: Anhydrous salts	Quantity (g)	Molar concentration in the final medium
MgCl ₂ 6H ₂ O	95.920	4.71 x 10 ⁻²
CaCl ₂ 2H ₂ O	13.440	9.14 x 10 ⁻³
SrCl ₂ 6H ₂ O	0.218	8.18 x 10 ⁻⁵

Table 3: BG11 media stocks (added to artificial seawater to produce media) developed by (Allen and Stanier, 1968) and modified by (Watanabe et al., 2000). The nutrient stocks were prepared by Alyson MacCormack and stored in a standard laboratory refrigerator to minimize deterioration.

Component	Stock Solution (g L ⁻¹ dH ₂ O)	Quantity to Media (mL)	Molar Concentration in Final Medium
NaNO ₃	149.6	10	1.76 x 10 ⁻²
MgSO ₄ • 7H ₂ O	75.0	1	3.04 x 10 ⁻⁴
CaCl ₂ • 2H ₂ O	27.0	1	1.84 x 10 ⁻⁴
Na ₂ CO ₃	20.0	1	1.89 x 10 ⁻⁴
Fe Citrate solution	—	1	—
Citric acid	6.0	—	3.12 x 10 ⁻⁵
Ferric ammonium citrate	6.0	—	~ 3 x 10 ⁻⁵
Na ₂ EDTA • 2H ₂ O	0.8413	1	2.26 x 10 ⁻⁶
K ₂ HPO ₄	39.0	1	2.24 x 10 ⁻⁴
Trace metal solution	See Table 4	1	—

Table 4: BG11 trace metal stock solution protocol developed by (Allen and Stanier, 1968) and modified by (Watanabe et al., 2000). The solution was prepared by Alyson MacCormack and stored in a standard laboratory refrigerator to minimize deterioration.

Component	Stock Solution (g L ⁻¹ dH ₂ O)	Quantity to Media	Molar Concentration in Final Medium
H ₃ BO ₃	—	2.860 g	4.63 x 10 ⁻⁵
MnCl ₂ • 4H ₂ O	—	1.810 g	9.15 x 10 ⁻⁶
ZnSO ₄ • 7H ₂ O	—	0.220 g	7.65 x 10 ⁻⁷
CuSO ₄ • 5H ₂ O	79.0	1 mL	3.16 x 10 ⁻⁷
Na ₂ MoO ₄ • 2H ₂ O	—	0.391 g	1.61 x 10 ⁻⁶
Co(NO ₃) ₂ • 6H ₂ O	49.4	1 mL	1.70 x 10 ⁻⁷

Experimental protocol

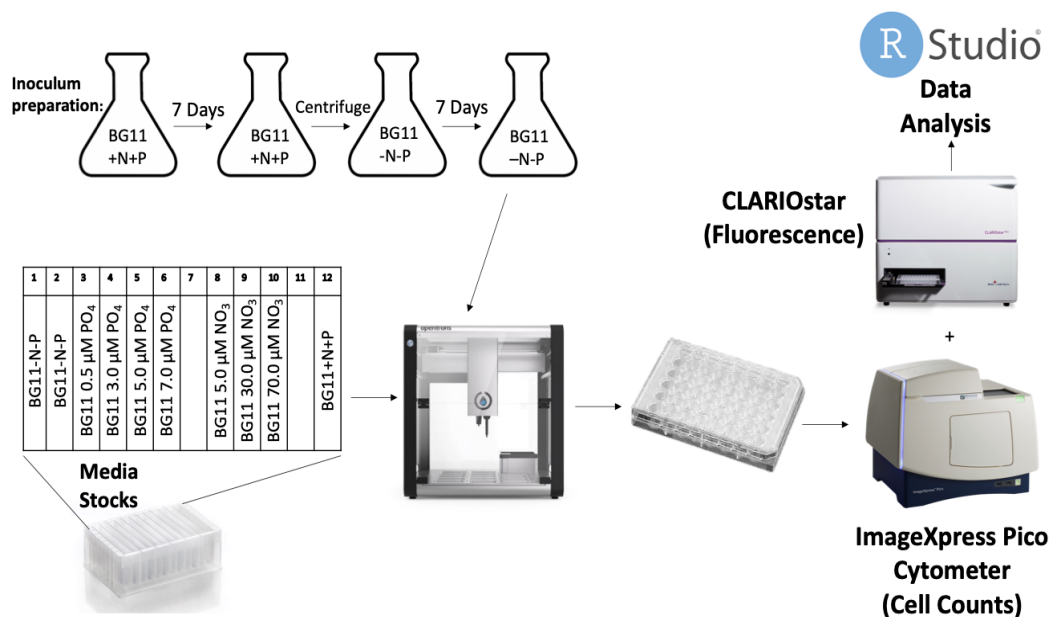


Figure 1: Experimental workflow schematic.

Inoculation Culture Preparation

Before starting a new experimental run, mother culture samples for each strain needed to be introduced to NO₃ and PO₄ depletion. Experimental culture creation required taking 5 mL of mother culture and adding it to 50 mL of the nitrogen and phosphorus replete BG11 media of the salinity corresponding to each strain. These cultures were grown in an Erlenmeyer flask on a shake plate inside a 22°C incubator with a 12:12 light to dark photoperiod and 100 μmol photons m⁻²s⁻¹ of light. After allowing the cultures to grow and build up for a week, they were then transferred to nitrogen and phosphorus depletion to initiate the metabolism of nitrogen and phosphorus stores. The transferring protocol is as follows:

1. The initial cultures were first transferred to 50 mL falcon tubes and centrifuged in a Beckman Coulter Avanti J-20 at 3241 rpm (2400 RCF) for 10 minutes.
2. Once a pellet formed, the nutrient replete media was removed using a stereological pipet and replaced with 50 mL of nitrogen and phosphorus deplete (N-P-free) BG11 media, and the culture was resuspended with shaking.
3. Steps 1 and 2 were then repeated.

Once the cultures were moved into nutrient-depleted conditions, they were once again grown for a week in the same environmental conditions as before to allow them to activate a nutrient-stress reaction and metabolize the nitrogen and phosphorus stores they had reserved.

Controlled Culturing

This study aimed to examine the growth of picocyanobacteria in a set gradient of five phosphorus (0 μM , 0.5 μM , 3.0 μM , 5.0 μM , and 7.0 μM) and four nitrogen concentrations (0 μM , 5.0 μM , 30.0 μM , and 70.0 μM), the organization of which is displayed in figure 2. To create the experimental nutrient matrices, 175000 μmolL^{-1} nitrogen and 17500 μmolL^{-1} phosphorus nutrient stocks diluted 100-fold with autoclaved Milli-q were mixed with nitrogen and phosphorus-deplete BG11 based on calculated ratios to create 12.5, 75, 125, and 175 μmolL^{-1} stocks of PO_4 and 125, 750, and 1750 μmolL^{-1} stock of NO_3 . Based on dilution ratios created for adding media and culture samples to the well plate, the nitrogen and phosphorus concentrations would balance out to the experimentally relevant values outlined in Figure 2. Once these nutrient stocks were prepared, a micro stir bar was placed inside each well of six 48 well plates, and then the plates were loaded inside the Opentrons robot (Model: OT2, Opentrons, Brooklyn, NY). Before proceeding, the inoculum cultures were cell counted with the Molecular Devices Imagexpress Pico Cytometer and with a hemocytometer and microscope. Once the cell counts were determined, each culture was diluted to a consistent initial population density using nutrient-depleted media. The Opentrons robot was used to add the media of varying nitrogen and phosphorus concentrations and diluted strain inoculant to each plate. Every 48 well plate carried wells with two different strains that required media of different salinities to limit the chance of cross-contamination across strains. Two millilitres of each nutrient stock mentioned above was mixed with 20 mL of N-P-free media and placed into designated storage troughs, the organization of which can be found in the experimental protocol diagram. The Opentrons robot placed media and culture inoculum in the wells at a ratio of 4:1, respectively (which was 941.2 μL of media and 235.3 μL per well in this

case) and created the experimental nutrient matrix shown in Figure 2. Once each of the plates was inoculated, they were then wrapped in parafilm and placed in a 22°C incubator with a 12:12 photoperiod, with each strain being exposed to 30, 100 and 300 $\mu\text{mol photons m}^{-2} \text{ s}^{-1}$ of light. Parafilm was used to prevent any loss or evaporation from well volume during the length of the experiment. A consistent, well volume is important for calculating culture density based on changes in culture dilution or concentration. Each culture was monitored and measured once a day for about two weeks, using the methods outlined in data collection. Following a run, the cultures were killed with bleach and disposed of.

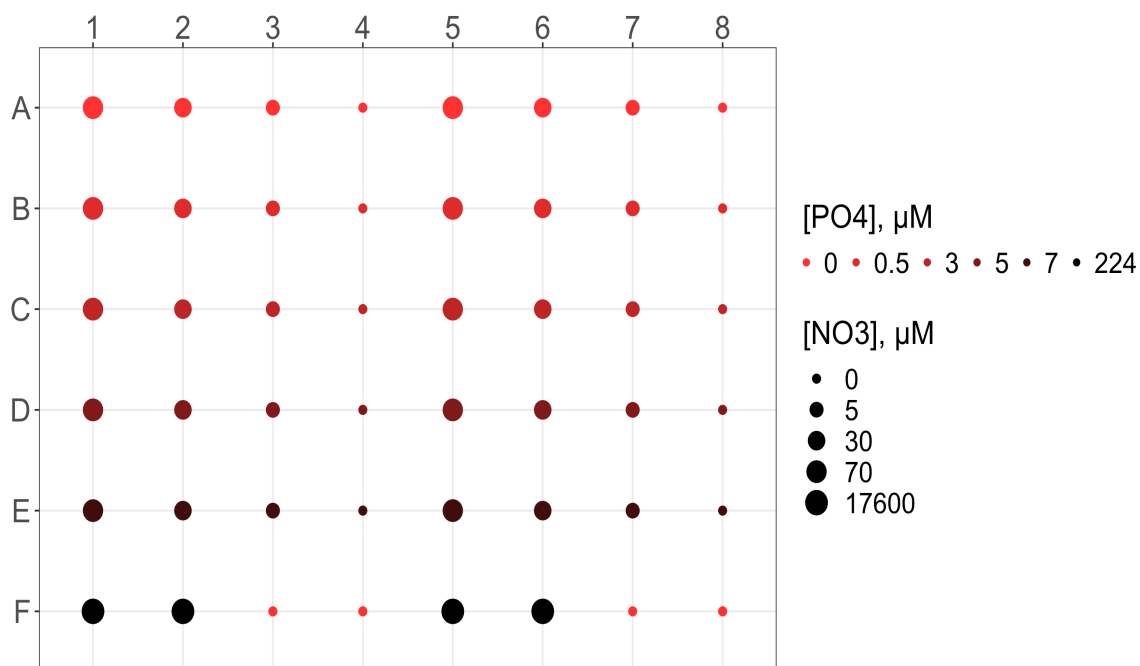


Figure 2: Well media concentrations used for controlled culturing experimental examination. Each plate contained two separate picocyanobacteria strains during trials. One strain would be contained in columns 1 to 4, and the second strain, with a different media salinity, was grown in columns 5 to 8. Final nitrate concentration is represented by point size, and final phosphate corresponds to point colour. The nutrient matrices are duplicates for each strain.

Data Collection

During the experimental run, culture growth for each well was examined daily. Both cell counts and fluorescence were used as growth proxies. The plates were centrifuged at 2000 rpm for 5 minutes in the Beckman Coulter Avanti J-20. For cell count determination, a Molecular Devices Imagexpress Pico Cytometer was used. The cytometer uses a fluorescence microscopic approach to provide cell counts, which means the cells need to be concentrated in one focal plane, or they will go undetected. Centrifuging the plates pulls the cultures to the bottom of each well to allow for more accurate imaging. Cell count data represents the cell count of 1% of the well's growth area (~cells/0.05 mL) and, through calculations, was used to represent culture density (cells/mL). Cell count data is represented in figures 1, 2, and 3 in the appendix. All data collected for this experiment was immediately uploaded to a cloud server, assembled with metadata, and visualized using RStudio version 1.4.1717.

Data Analysis

All experimental data files and analyses notebooks were compiled in an online repository. RStudio version 1.4.1717 was used to complete all data management and analysis. The tidyverse framework (Wickham et al., 2019) was used for most initial data compilation and modelling. The ARTool (Kay et al., 2021), emmeans (Lenth et al., 2021) and Vegan (Oksanen et al., 2020) packages were used for statistical analyses.

Importing Data

An R Notebook produced by Maximilian Berthold was used to import the cell count data collected and analyzed with the Imagexpress Pico Cytometer (Molecular Devices, San Jose, CA).

Data Modeling and Analyses

To detect differences in nutrient demand, significant distinct variations must be found between the growth of each strain in the experimental conditions. The cell counts collected for each strain were modelled using a non-linear Modified Gompertz approach. Modified Gompertz values were filtered for growth rate and placed into wide-format grouped by nutrient and light conditions, organized by strain. The dataset did not pass parametric assumptions, so a non-parametric approach was implemented. Between strains variation was modelled using a distance matrix visualized as a Non-metric Multi-dimensional Scaling (NMDS) plot and analyzed using an analysis of Similarities (ANOSIM). Within-strain, variation was modelled and analyzed using an aligned ranks transform analysis of variation (ART ANOVA). Each model examined the growth of each strain as separate dependent variables against the three independent variables: light level, nitrogen concentration, and phosphorus concentration.

Model for Between Strain Comparisons

Using the Bray Curtis approach to create a distance matrix for the Modified Gompertz growth rates, an NMDS ordination was produced using the vegan package for R. Using the analysis of similarities (ANOSIM) function allows for the detection of dissimilarities between strains based on nitrogen concentrations, phosphorus concentrations and light levels. If a significant difference was detected, the Similarity Percentages (SIMPER) test allowed us to determine which strain was the greatest driver of the variation. The creation of these NMDS plots and comparisons with ANOSIM is based on the tutorials created by Zorz (2019).

Model for Within-Strain Comparisons

Based on the approaches developed by Salvatore S. Mangiafico (Mangiafico, 2016), within-strain variation was examined using an Aligned Ranks Transformation (ART) ANOVA approach. The ARTool package allows ART ANOVAs to be conducted within the R framework. When creating this model, the dataset must include all independent and dependent variables and all interactions. The data is not required to be normally distributed but must adhere to additional assumptions for this nonparametric approach. Once the model is created, all aligned ranks must sum to zero, and the model must provide F values of ~ 0 and P values of ~ 1 to prevent variation created by the model itself. An Aligned Ranked Transform Contrasts (art.con) post-hoc comparison test represented the main effects for each strain with or without factor interactions.

Results

Identifying nutrient-dependent maximum growth duration and culture densities

Generally, nutrient levels appeared to influence overall cell counts and growth but demonstrated enough variation that trends became challenging to identify. Despite this, a combination of nutrient and strain-specific interactions emerged from the visualization of the data set. Nitrogen demonstrated its necessity for maximum growth duration (days) and cell density. For CZS48M and PCC6803, a general increasing growth duration and culture density trend accompanies increasing nitrogen concentrations. CZS25K appears to be an exception in this case due to its demonstration of minimal or no growth in samples examined in media with the nitrogen repletion but phosphorus depletion.

Compared to the observations for nitrogen, phosphorus appears to provide slightly more variation. CZS25K seemingly demonstrates the most significant phosphorus dependency between the three strains. Minimal or no growth appeared in multiple CZS25K samples with high nitrogen availability but phosphorus limitation or depletion. Phosphorus limitation appeared to induce more minor influences on CZS48M and PCC6803. Cultures of CZS48M generally maintained the ability to grow for an extended period but produced cultures with lowering densities based on phosphorus availability. PCC6803 exhibited negligible influence by a lack of environmental phosphorus, demonstrating minor variability based on phosphorus concentration but generally increasing alongside environmental nitrogen availability.

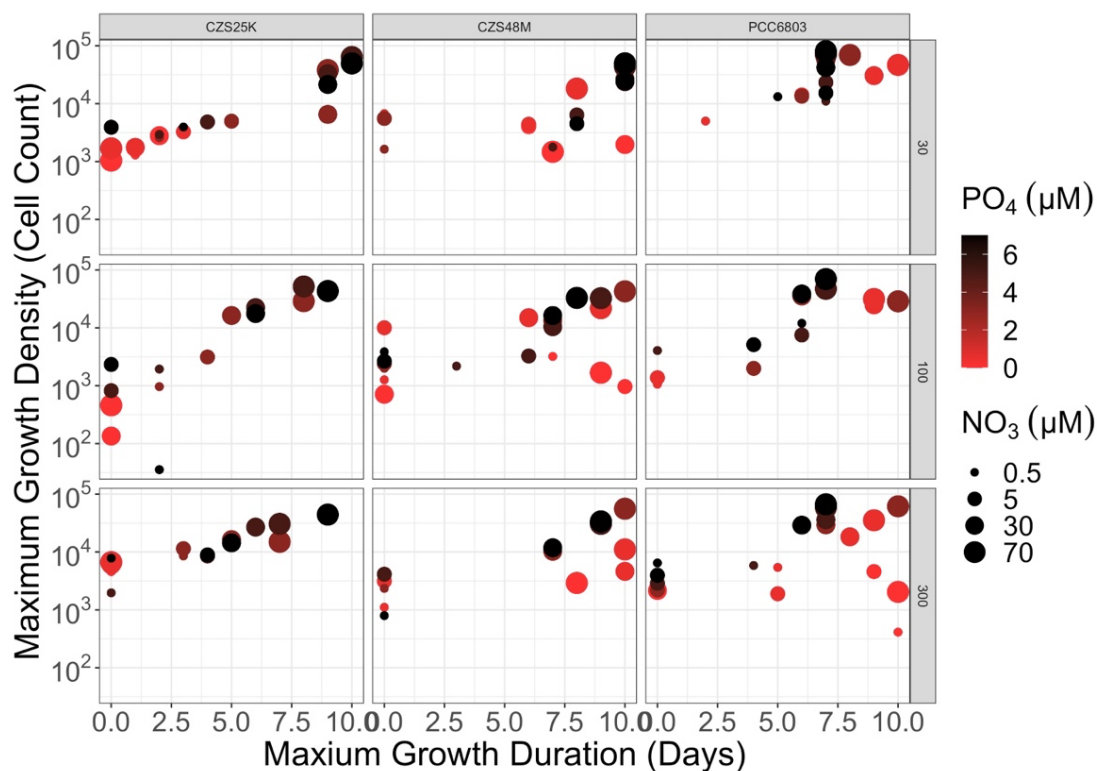


Figure 3: Metrics of maximum growth duration (cell count) and duration (days) created using rolling changes in cell counts from daily measurements. Nitrate concentration (μM) is represented by data point size, and phosphate concentration (μM) is a continuous numeric colour gradient.

Between Strain Nutrient Comparison

Creating an NMDS ordination for growth rates determined by a Modified Gompertz growth approach (Figure 5) produced a stress value of 0.1776016, which is lower than the optimum, generally considered to be values less than 0.2. The only independent variable to cause a significant variation between strains, in this case, was NO₃ (μM), with a significance value of 0.0011 and an R statistic of 0.03731. Post-hoc comparisons showed no variation driven by CZS25K. CZS48M demonstrated the highest differences in growth rate for NO₃ comparisons of 0 μM and 30 μM . Finally, PCC6803 was the dominant driver among all other NO₃ level comparisons.

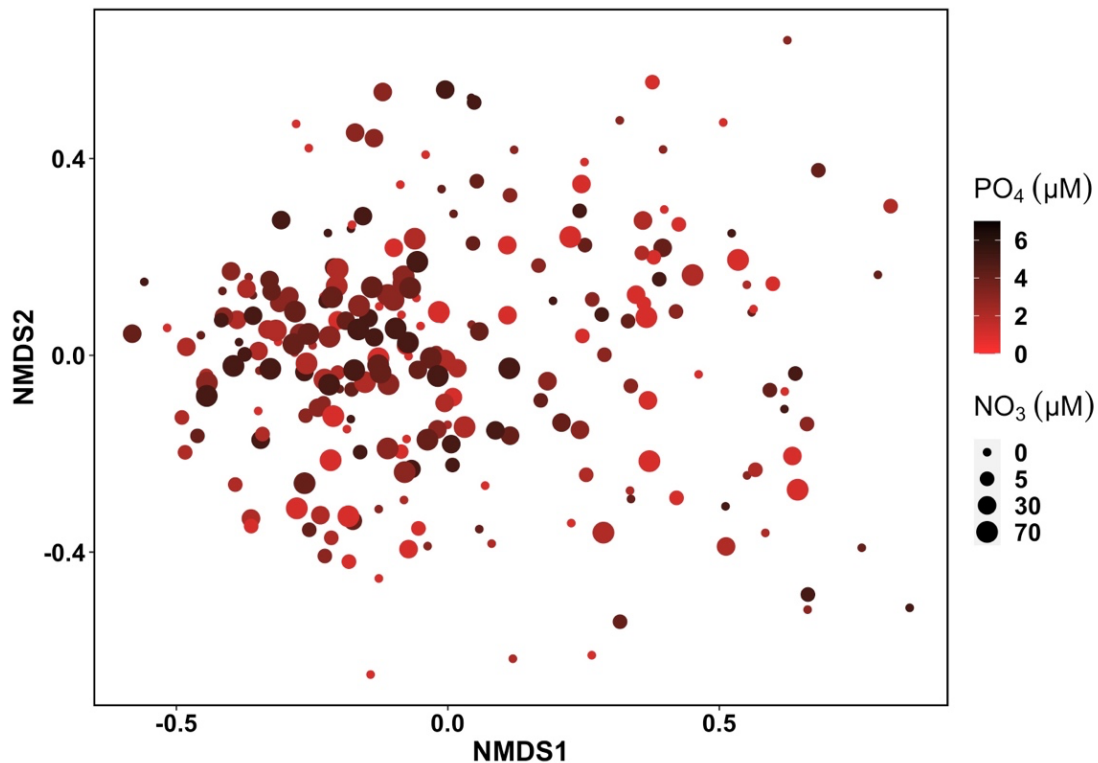


Figure 4: Non-metric Multi-dimensional Scaling (NMDS) created with a bray Curtis distribution to represent strain growth rates modelled by a Modified Gompertz equation, used to model between strain variation based on nutrient concentration. Nitrate concentration (μM) is represented by data point size, and phosphate concentration (μM) is a continuous numeric colour gradient.

Within-Strain Nutrient Comparison

Within-strain comparisons were made using an ART ANOVA and Aligned Ranked Transform Contrasts (art.con) post-hoc comparison test approach. ART ANOVA modelling assumes that all aligned ranks will sum to zero, and the model must provide F values of about 0 and P values of around 1 to prevent variation created by the model itself. Below are the results of interpreting strain growth rates using a Modified Gompertz approach on cell count data.

CZS25K

The model created sums for CZS25K's aligned ranks that perfectly summed to zero, but not all F and P values met assumptions. All the F values for the Modified Gompertz were below 0.0420066. Overall, most of the aligned ranks p-values for the model were 1, and the value demonstrating the greatest deviation was 0.97728. Despite a lack of complete F and P value assumptions adherence, the model still falls within a range where ART ANOVA interpretation is reasonable with the inclusion of this acknowledgement. The main effects of this model showed significance for NO₃ (P = 2.1652e-5) and PO₄ (P = 0.0027305) but also produced a significant interaction of nitrogen and phosphorus (P = 0.0001824) with no apparent impact or interactions based on light levels. Below Modified Gompertz growth rates are visualized (Figure 5), and post hoc comparisons with relative or borderline significance are represented (Table 5).

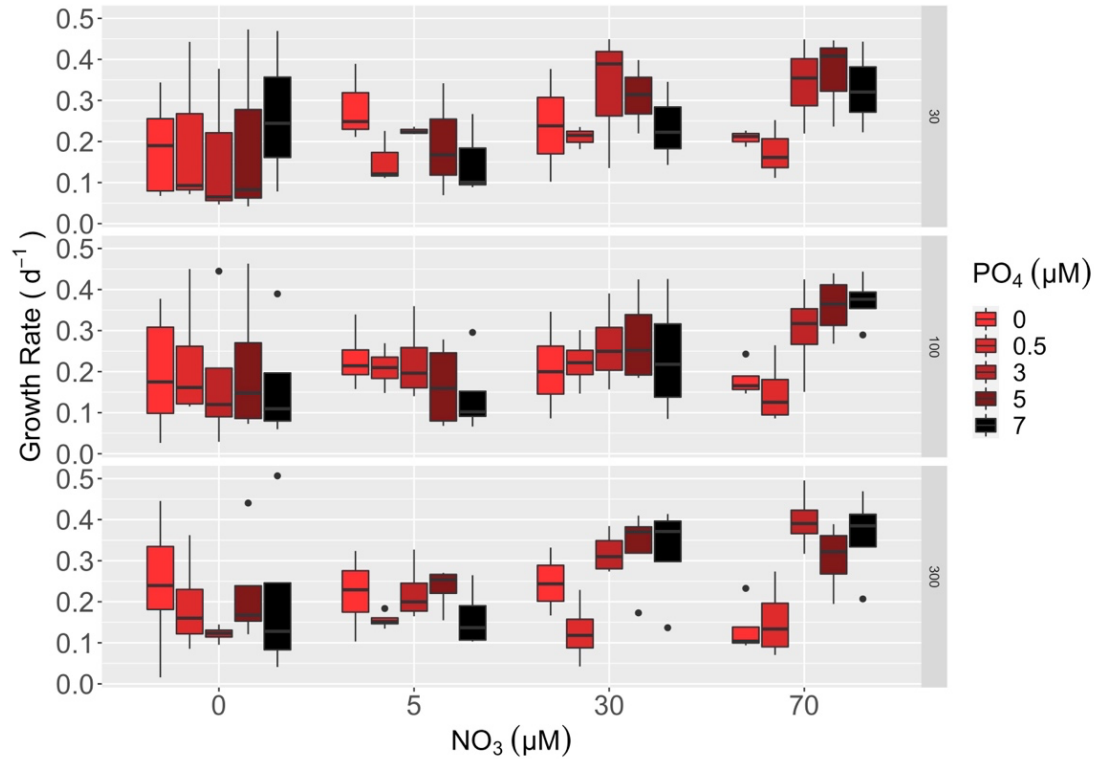


Figure 5: Boxplot representation of CZS25K growth rates produced using the Modified Gompertz equation to create a growth rate metric using cell counts collected to monitor culture-specific growth. The data is divided by nitrate concentration and organized for side-by-side phosphorus comparisons within each level of NO_3 . Row faceting represents changes in light intensity ($\mu\text{mol photons m}^{-2} \text{s}^{-1}$).

Table 5: Post hoc comparison created using an ARTool Aligned Ranked Transform Contrasts (art.con) approach. One factor and interaction nutrient comparisons organized by column are represented for CZS25K.

Nitrate Contrasts (μM)	Phosphate Contrasts (μM)	Pairwise Interaction Contrasts (NO_3, PO_4) (μM)	P- Value
0 - 30	—	—	0.0068
0 - 70	—	—	0.0003
5 - 30	—	—	0.0213
5 - 70	—	—	0.0012
—	0.5 - 3	—	0.0062
—	0.5 - 5	—	0.0081
—	0.5 - 7	—	0.0522

Nitrate Contrasts (μM)	Phosphate Contrasts (μM)	Pairwise Interaction Contrasts (NO_3, PO_4) (μM)	P- Value
—	—	0,0 - 70,7	0.0625
—	—	0,0.5 - 70,3	0.1810
—	—	0,0.5 - 70,5	0.2021
—	—	0,0.5 - 70,7	0.1178
—	—	0,3 - 30,3	0.1573
—	—	0,3 - 30,5	0.1199
—	—	0,3 - 70,3	0.0125
—	—	0,3 - 70,5	0.0148
—	—	0,3 - 70,7	0.0067
—	—	0,5 - 70,3	0.1697
—	—	0,5 - 70,5	0.1898
—	—	0,5 - 70,7	0.1096
—	—	0,7 - 70,3	0.2099
—	—	0,7 - 70,5	0.2333
—	—	0,7 - 70,7	0.1388
—	—	30,0.5 - 70,3	0.1937
—	—	30,0.5 - 70,5	0.2159
—	—	30,0.5 - 70,7	0.1270
—	—	30,3 - 5,7	0.1136
—	—	30,3 - 70,0.5	0.2103
—	—	30,5 - 5,7	0.0849
—	—	5,0.5 - 70,3	0.0996
—	—	5,0.5 - 70,5	0.1131
—	—	5,0.5 - 70,7	0.0612
—	—	5,5 - 70,3	0.2812
—	—	5,5 - 70,7	0.1929
—	—	5,7 - 70,3	0.0079
—	—	5,7 - 70,5	0.0094
—	—	5,7 - 70,7	0.0042

Nitrate Contrasts (μM)	Phosphate Contrasts (μM)	Pairwise Interaction Contrasts (NO_3 , PO_4) (μM)	P- Value
—	—	70,0 - 70,3	0.0683
—	—	70,0 - 70,5	0.0782
—	—	70,0 - 70,7	0.0407
—	—	70,0.5 - 70,3	0.0191
—	—	70,0.5 - 70,5	0.0224
—	—	70,0.5 - 70,7	0.0105

Visualizing the growth rates of CZS25K as a box plot (Figure 5) demonstrated multiple possible trends. To start with phosphate concentrations of 3, 5 and 7 μM , the average growth rate increased with every rise in nitrogen concentration. In phosphate depletion or deficiency (0 and 0.5 μM), no samples demonstrated an average growth rate above $\sim 0.25 \text{ d}^{-1}$. In addition to this, phosphorus depletion consistently produced a higher average growth rate than phosphate deficiency (0.5 μM). Excluding growth rate for total nutrient deficiency (NO_3 and PO_4), cultures with only phosphate depletion or deficiency generally saw an increase in average growth rate accompanying rises in nitrate, except for the cultures examined with lower phosphate concentration and nitrate saturation (70 μM) which produced average growth rates which were more similar to those observed in nitrate deficiency or depletion (0 and 5 μM) than that observed in 30 μM of nitrate.

An ART approach mirrored the findings of the NMDS approach, similarly describing nitrogen's influence on the growth rate of CZS25K. Post hoc comparisons showed that the growth rate of CZS25K was significantly altered based on the presence of either total nitrate depletion or relative stress-inducing deficiency. Distinctly CZS25K was the only strain to show growth rate variation based on phosphate concentrations. Post

hoc comparisons demonstrated that the growth of CZS25K was significantly inhibited or reduced by depleted or limited phosphate concentrations. An art model for the strain demonstrates a highly significant interaction between nutrient concentrations. Post hoc comparisons of interaction combinations demonstrated that most of this variation was produced by similar drivers represented in the main effects.

CZS48M

The sums of the Modified Gompertz model created for CZS48M had aligned ranks that summed to zero, but the aligned ranks F and P values failed to meet assumptions. The highest F value for the Modified Gompertz was 0.0872543. Most p-values were equal to 1, but the greatest deviation was 0.96696. The models were again still interpreted due to assumptions falling within a reasonable range of adherence. The main effects of the Modified Gompertz model showed significance for NO_3 ($P = 0.00556181$), PO_4 ($P = 0.04653405$), and light level ($P = 0.00040646$) but also produced a significant interaction of nitrogen and phosphorus ($P = 0.02688589$) with no apparent interactions based on light levels. Below Modified Gompertz growth rates are visualized (Figure 6), and post hoc comparisons with relative or borderline significance are represented (Table 6).

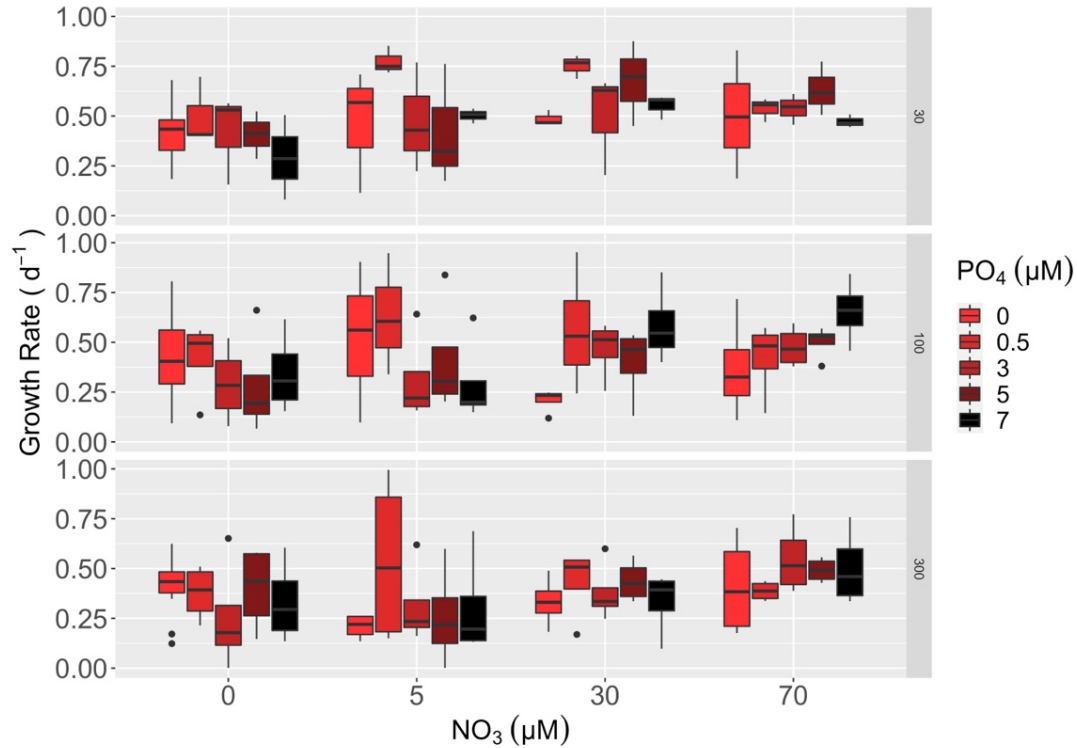


Figure 6: Boxplot representation of CZS48M growth rates produced using the Modified Gompertz equation to create a growth rate metric using cell counts collected to monitor culture-specific growth. The data is divided by nitrate concentration and organized for side-by-side phosphorus comparisons within each level of NO_3 . Row faceting represents changes in light intensity ($\mu\text{mol photons m}^{-2} \text{s}^{-1}$).

Table 6: Post hoc comparison created using an ARTool Aligned Ranked Transform Contrasts (art.con) approach. One factor and interaction nutrient comparisons organized by column are represented for CZS48M.

Nitrate Contrasts (μM)	Phosphate Contrasts (μM)	Light Level Contrasts (μe)	Pairwise Interaction Contrasts (NO_3 , PO_4) (μM)	P-Value
0 - 30	—	—	—	0.0928
0 - 70	—	—	—	0.0113
5 - 30	—	—	—	0.2682
5 - 70	—	—	—	0.0542
—	0 - 0.5	—	—	0.0446
—	0.5 - 3	—	—	0.0708
—	—	30 - 100	—	0.0188
—	—	30 - 300	—	0.0003
—	—	—	0,3 - 5,0.5	0.2837
—	—	—	30,0 - 5,0.5	0.2268

Like CZS25K, CZS48M visualization (Figure 6) revealed a fairly consistent increase in average growth rate for cultures with higher phosphate availability (concentrations of 3, 5, and 7 μM) as nitrate concentrations increased beyond 5 μM . However, these three-phosphate concentrations demonstrated no major growth rate changes between different concentrations within each level of nitrate. The growth rates of cultures with higher phosphate availability generally remained the same between nitrogen levels of depletion or deficiency (0 and 5 μM). The growth rate findings for phosphate levels 0 and 0.5 μM demonstrated major differences between nitrate concentrations. Making distinguishing trends, outside of growth rates for 0.5 μM phosphate being consistently higher than that of phosphate 0 μM cultures, difficult to identify and convey.

CZS48M showed to be distinctly sensitive compared to the other two strains in this analysis. As with CZS25K growth rate between and within-strains was significantly

influenced by the abundance of environmental nitrate. In addition to variation driven by environmental nitrate, CZS48M was the only strain that exhibited variation induced by light level. In this case growth rate was influenced by the lowest light level compared to both higher concentrations. The phosphate analysis findings were unexpected. In contrast to all other comparisons, CZS48M produced growth rate variation between phosphate depletion and deficiency levels instead of the common contrasts of deficiency and abundance.

PCC6803

The sums of the model created for PCC6803 had aligned ranks that summed to zero but again failed to meet F and P-value assumptions. The highest F value for the Modified Gompertz model was 2.088e-01. Overall, most of the aligned ranks' p-values were 1, but the Modified Gompertz greatest deviation was 0.93330. The models were still interpreted due to sum assumption adherence and F and P values within a reasonable range of 1 and 0. The main effects Modified Gompertz model showed significance for NO_3 ($P = 0.00021022$) and borderline significance for PO_4 ($P = 0.09990434$) with no interactions based on nutrient or light levels. Below Modified Gompertz growth rates are visualized (Figure 7), and post hoc comparisons with relative or borderline significance are represented (Table 7).

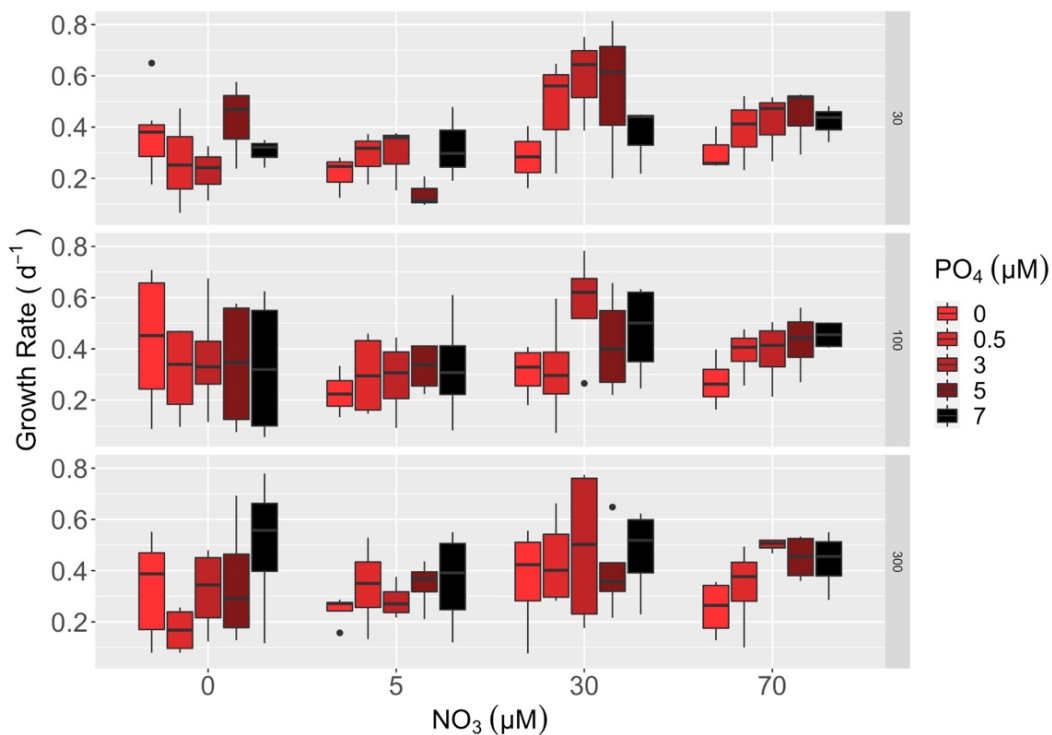


Figure 7: Boxplot representation of PCC6803 growth rates produced using the Modified Gompertz equation to create a growth rate metric using cell counts collected to monitor culture-specific growth. The data is divided by nitrate concentration and organized for side-by-side phosphorus comparisons within each level of NO_3 . Row faceting represents changes in light intensity ($\mu\text{mol photons m}^{-2} \text{s}^{-1}$).

Table 7: Post hoc comparison for PCC6803. It was created using an ARTool Aligned Ranked Transform Contrasts (art.con) approach. There are representations of one-factor nutrient comparisons with the absence of an interaction, organized into columns based on nutrient type (nitrate or phosphate).

Nitrate Contrasts (μM)	Phosphate Contrasts (μM)	P-Value
0 - 5	—	0.1806
0 - 30	—	0.0829
5 - 30	—	0.0002
5 - 70	—	0.0062
—	0 - 3	0.2554
—	0 - 7	0.2116

Visuals for PCC6803 growth rates (Figure 7) demonstrate an array of nutrient-based variations making trends challenging to distinguish. Generally, growth rates appeared to increase as nitrate and phosphate levels became higher, except for the culture with a deficiency of both. In addition, growth rates suggest a possible point of nitrogen saturation with subtle growth rate decreases when moving from a concentration of 30 μM to 70 μM . In addition, the growth rate appeared to be slightly inhibited by phosphate concentrations less than 0.5 μM for nitrate conditions between 5 μM and 30 μM . Phosphate also demonstrates a possible saturation point (with a nitrate concentration of 70 μM) as the growth rate appears to decrease when moving from 5 μM to 7 μM phosphate.

PCC6803 statistically represented the lowest sensitivity to nutrient and light-related stress. The only independent variable to produce a growth response was nitrate concentration. The growth rate of PCC6803 determined using cell count as a growth proxy was inhibited in conditions with nitrate deficiency or deficit.

Discussion

General Findings

Monitoring the nutrient usage and determining growth niches using an NMDS and ART ANOVA-based approach appears to be an effective method of demonstrating between and within-strain variability concerning changes in nitrate, phosphate and light levels within experimental cultures. The *Cyanobium* strains (CZS25K & CZS48M) demonstrated significant interactions of nitrate and phosphate. Meanwhile, no notable interactions were detected for *Synechocystis* (PCC6803). In general, comparisons based on nutrient interactions produced similar contrasts to those represented by the main effects but were more difficult to represent in a multivariate context. General trends showed growth rates were influenced, both within and between strains, based on nitrate availability. In addition, CZS25K demonstrated the most distinct phosphate influence, and CZS48M growth was additionally modified by light intensity.

Out of the three experimental subjects, CZS48M was distinctly sensitive to the greatest number of independent factors. Furthermore, CZS48M was the only strain to present a unique challenge to collecting daily readings during experimentation. CZS48M cultures continually developed aggregates throughout experimental trials, which posed the risk of skewing growth measurements. Previous studies have demonstrated that clumping is used as an algal stress response to conditions like nutrient stress (Yan et al., 2021). Considering these peculiar findings, future studies should examine if nutrient stress influences the creation of clumping within picocyanobacteria like *Cyanobium*, which includes CZS48M.

Relevance of Findings

The usage of nutrients by phytoplankton has been most commonly understood by the Redfield ratio for most of the past 100 years. The Redfield ratio states that phytoplankton biomass almost consistently contains a ratio of carbon to nitrogen to phosphorus that is 106:16:1 (Redfield, 1934). This ratio was published in 1934, so it is still not well understood what impacts modern water body eutrophication will have on the usage of nitrogen and phosphorus by phytoplankton for growth (Shangguan et al., 2017). Many studies have shown that phytoplankton can adapt to these increases in nutrients for the continued growth of additional biomass, even reacting by modifying their nutrient usage or changing their elemental ratios such as carbon:nitrogen in the case of phosphorus deficiencies (Xu et al., 2010; De Senerpont Domis et al., 2014). Further studies have shown that as phytoplankton communities adapt to human-induced environmental changes, like large-scale nutrient influx, cyanobacteria appear to have the greatest ability to adapt and assume dominance within phytoplankton communities (Elliott et al., 2006). With their ability to increase nutrient uptake and benefit from a decrease in packing effect due to their small cell size and thinner cell membranes, picocyanobacteria are uniquely equipped to dominate in specific conditions such as nutrient deficiencies that are unable to sustain the growth or survival of larger cyanobacteria strains (Raven, 1998).

Strain-specific nutrient usage is likely to be primarily regulated by nutrient uptake and storage mechanisms. Cyanobacteria most commonly use polyphosphates as the phosphorus storage product and phycobilin protein pigments to store nitrogen (Kromkamp, 1987). A microbe's ability to uptake nutrients is greatly dependent on nutrient usage and levels within internal stores (Kromkamp, 1987). Using this theory for

situations of nutrient stress, microorganisms should be able to survive on nutrient stores accumulated during periods of abundance, and strains with greater storage capacity should have a greater chance of survival (Dawes and Senior, 1973). A reliance on nitrogen by picocyanobacteria is seemingly demonstrated by shifts to the use of increased carbon to nitrogen ratios in phosphorus deficiency, but what occurs when aquatic environments experience nitrogen limitation instead (Xu et al., 2010; De Senerpont Domis et al., 2014). Studies have demonstrated that picocyanobacteria like *Synechococcus* can enact phenotypic responses to weaken the influence of nitrogen limitation, including using nitrate, nitrite, urea, cyanate, and amino acids as their nitrogen source (Palenik et al., 2003; Lindell et al., 2005). During the week that the cultures of this experiment underwent both nitrate and phosphate depletion, a lack of both nutrients in any form likely rendered the cell nutrient limitation mechanisms useless, creating a forced reliance on the metabolism of nutrient stores for survival. While picocyanobacteria are still bound to these concepts, they have many unique adaptations introducing major nutrient uptake and usage changes. As mentioned before, picocyanobacteria benefit from their small size because of a reduction in the packing effect, which allows for survival on much lower levels of nutrient influx, which is beneficial for culture growth and maintenance during nutrient limitation or fixation (Raven, 1998). In addition, nutrient uptake of picocyanobacteria can occur much faster due to a higher surface area to volume ratio and increased diffusion efficiency from thinner cell membranes in the environment (Raven, 1998). These adaptations give picocyanobacteria an advantage over larger forms of phytoplankton, but what drives survival between strains of a smaller size? Smaller forms of phytoplankton typically prioritize nutrient and light uptake usage efficiency.

This is exhibited by the nutrient adaptations already mentioned and having generally greater chlorophyll densities and light absorption capacities (Agustí, 1991a; Finkel et al., 2004; Wu et al., 2014). With phycobilin proteins known to be used for nitrogen storage, greater chlorophyll abundance likely supports the idea that picocyanobacteria favour the efficiency of nutrient usage over storage capacity (Kromkamp, 1987). The study included collecting fluorescence data to examine phycobilisome to chlorophyll ratios but remains unevaluated. Therefore, its analysis will become the focus of future research. Within the experimental strains, PCC6803 is larger than the *Cyanobium* strains. *Cyanobium* is generally considered to measure less than 2 μM , with the examples found by (Albrecht et al., 2017) measuring at $\sim 1.63 \mu\text{m}$ in diameter for CZS25K and $\sim 1.2 \mu\text{m}$ for CZS48M. *Synechocystis* PCC6803 has been measured to have diameters between $1.96 \pm 0.03 \mu\text{m}$ to $2.19 \pm 0.03 \mu\text{m}$ which are higher than the *Cyanobium* strains but still within the 3 μm classification for picocyanobacteria (Jasser and Callieri, 2016; Zavřel et al., 2018). PCC6803 is also the only strain to exhibit no variation induced by phosphate limitation. Based on this, future studies should explore if there are strain-specific trade-offs between storage capacities and usage efficiency based on the cell size of picocyanobacteria. Such a trade-off could help to account for the overall greater sensitivity of the smaller *Cyanobium* strains to nutrient abundance following a period of limitation in comparison to the larger cells of PCC6803.

The results of this study generally agree with the changes to nutrient usage mechanisms established within previous literature. For these strains, the growth rate generally increased with a higher abundance of nitrate and phosphate within each culture. As the statistics show, nitrogen appears to act as the major limiting factor for all three

strains, while CZS48M and PCC6803 had some capacity to survive in differing conditions of phosphorus deficiency. This echoes the findings of De Senerpont Domis et al. (2014), which demonstrated phytoplankton's capacity to adapt their carbon:nitrogen ratios in response to environmental declines of phosphate. This study focused on nitrate as the major nitrogen substrate used in picocyanobacterial growth, but studies examining picocyanobacterial usage of alternative nitrogen sources help support an overall nitrogen dependency. Many studies have shown that ammonium is the preferred nitrogen source of many forms of phytoplanktons because of lower assimilation costs, but increasing levels of NH_4^+ within an environment can induce a limiting effect on phytoplankton growth (Dortch, 1990; Dugdale et al., 2007; Collos and Harrison, 2014; Glibert et al., 2016, 2021). Picocyanobacteria's small size prevents ammonium accumulation, and strains like *Synechococcus* are tolerant and uninhibited by high levels of NH_4^+ , allowing it to be continually used as a nitrogen substrate (Glibert et al., 2010, 2016, 2021; Collos and Harrison, 2014). This study demonstrates the importance of nitrogen to strains of *Cyanobium* and *Synechocystis* and the likelihood that they possess similar opportunistic mechanisms of nitrogen uptake like those seen in *Synechococcus* (Collos and Harrison, 2014; Glibert et al., 2021). Thus, support exists for pursuing either physiological or genotypic research into understanding the deeper mechanics of nitrogen usage and adaption for *Cyanobium* and *Synechocystis*.

Morphology changes are another primary consideration that must be made to understand how growth rate is influenced by nutrient availability. Previous studies have shown that when placed under grazing stress, *Cyanobium* was documented to undergo morphological changes that either began to resemble or were mistakenly identified as

larger strains like *Aphanothece* before undergoing genotypic identification (Jezberová and Komárková, 2007; Huber et al., 2017). This can occur from colony aggregation or mucilage (Albrecht et al., 2017) like those produced by CZS48M under nutrient stress for this experiment. The cell counts collected for this experiment were based on fluorescent signaling and did not include brightfield imaging. This study failed to incorporate a method with sensitivity high enough to monitor for changes in cell morphology or colony formation outside of the aggregations demonstrated by CZS48M. Therefore more in-depth evaluation is required to characterize *Cyanobium*'s response to environmental stress. Future studies should examine the influences of stress-induced *Cyanobium* aggregation on culture and colony nutrient usage. If stress-induced morphological changes produce nutrient-based physiological responses, this may significantly influence the growth rate that should be considered in the evaluation of *Cyanobium*'s nutrient usages.

The ability to identify and statistically support distinct differences in nutrient use between and within strains supports the effectiveness of using nutrient niche determination as an alternative method of strains characterization. The major downfall of this work is that the findings only provide information for the three strains involved and cannot be generalized to the greater cyanobacteria community. Nevertheless, the methodology of this study provides a practical method capable of being applied to examine nutrient uses within other strains. Identifying optimal initial inoculum density than expanding its role within the experimental methodology and adding a protocol to monitor for morphological adaptations would be beneficial. These adjustments would allow for more in-depth refinement of strain nutrient niches. These results contribute to a

greater understanding of picocyanobacteria's physiological responses to nutrient limitations. This understanding can help with mechanistic genomic characterizations and contribute to human knowledge on picocyanobacteria's usage and adaptation to their environment for global phytoplankton monitoring and management.

References

- Agustí, S. (1991a). Allometric Scaling of Light Absorption and Scattering by Phytoplankton Cells. *Can. J. Fish. Aquat. Sci.* 48, 763–767. doi: 10.1139/f91-091.
- Agustí, S. (1991b). Light environment within dense algal populations: cell size influences on self-shading. *Journal of Plankton Research* 13, 863–871. doi: 10.1093/plankt/13.4.863.
- Agusti, S., Duarte, C. M., and Canjield Jr., D. E. (1990). Phytoplankton abundance in Florida lakes: Evidence for the frequent lack of nutrient limitation. *Limnology and Oceanography* 35, 181–187. doi: 10.4319/lo.1990.35.1.0181.
- Albrecht, M., Pröschold, T., and Schumann, R. (2017). Identification of Cyanobacteria in a Eutrophic Coastal Lagoon on the Southern Baltic Coast. *Front. Microbiol.* 8. doi: 10.3389/fmicb.2017.00923.
- Allen, M., and Stanier, R. (1968). Growth and Division of Some Unicellular Blue-green Algae. *Journal of general microbiology* 51, 199–202. doi: 10.1099/00221287-51-2-199.
- Andersen, R., Berges, J., Harrison, P., and Watanabe, M. M. (2005). Appendix A - recipes for freshwater and seawater media. *Algal Culture Techniques*, 429–539.
- Anisfeld, S. C., Barnes, R. T., Altabet, M. A., and Wu, T. (2007). Isotopic Apportionment of Atmospheric and Sewage Nitrogen Sources in Two Connecticut Rivers. *Environ. Sci. Technol.* 41, 6363–6369. doi: 10.1021/es070469v.
- Berges, J. A., Franklin, D. J., and Harrison, P. J. (2001). Evolution of an Artificial Seawater Medium: Improvements in Enriched Seawater, Artificial Water Over the Last Two Decades. *Journal of Phycology* 37, 1138–1145. doi: <https://doi.org/10.1046/j.1529-8817.2001.01052.x>.
- Berthold, M., and Campbell, D. A. (2021). Restoration, Conservation and Phytoplankton Hysteresis. *Conservation Physiology* submitted.
- Collos, Y., and Harrison, P. J. (2014). Acclimation and toxicity of high ammonium concentrations to unicellular algae. *Marine Pollution Bulletin* 80, 8–23. doi: 10.1016/j.marpolbul.2014.01.006.
- Dawes, E. A., and Senior, P. J. (1973). “The Role and Regulation of Energy Reserve Polymers in Micro-organisms,” in *Advances in Microbial Physiology*, eds. A. H. Rose and D. W. Tempest (Academic Press), 135–266. doi: 10.1016/S0065-2911(08)60088-0.
- De Senerpont Domis, L. N., Van de Waal, D. B., Helmsing, N. R., Van Donk, E., and Mooij, Wolf. M. (2014). Community stoichiometry in a changing world:

- combined effects of warming and eutrophication on phytoplankton dynamics. *Ecology* 95, 1485–1495. doi: 10.1890/13-1251.1.
- Dortch, Q. (1990). The interaction between ammonium and nitrate uptake in phytoplankton. *Mar. Ecol. Prog. Ser.* 61, 183–201. doi: 10.3354/meps061183.
- Duan, S., Delaney-Newcomb, K., Kaushal, S. S., Findlay, S. E. G., and Belt, K. T. (2014). Potential effects of leaf litter on water quality in urban watersheds. *Biogeochemistry* 121, 61–80.
- Dugdale, R. C., Wilkerson, F. P., Hogue, V. E., and Marchi, A. (2007). The role of ammonium and nitrate in spring bloom development in San Francisco Bay. *Estuarine, Coastal and Shelf Science* 73, 17–29. doi: 10.1016/j.ecss.2006.12.008.
- Elliott, J. A., Jones, I. D., and Thackeray, S. J. (2006). Testing the Sensitivity of Phytoplankton Communities to Changes in Water Temperature and Nutrient Load, in a Temperate Lake. *Hydrobiologia* 559, 401–411. doi: 10.1007/s10750-005-1233-y.
- Finkel, Z. V., Irwin, A. J., and Schofield, O. (2004). Resource limitation alters the 3/4 size scaling of metabolic rates in phytoplankton. *Marine Ecology Progress Series* 273, 269–279. doi: 10.3354/meps273269.
- Flombaum, P., Gallegos, J. L., Gordillo, R. A., Rincón, J., Zabala, L. L., Jiao, N., et al. (2013). Present and future global distributions of the marine Cyanobacteria *Prochlorococcus* and *Synechococcus*. *Proc Natl Acad Sci U S A* 110, 9824–9829. doi: 10.1073/pnas.1307701110.
- Glibert, P., Boyer, J., Heil, C., Madden, C., Sturgis, B., and Wazniak, C. (2010). Blooms in Lagoons: different from those of river-dominated estuaries. *Coastal Lagoons: Critical Habitats of Environmental Change*, 91–114.
- Glibert, P. M., Heil, C. A., Madden, C. J., and Kelly, S. P. (2021). Dissolved organic nutrients at the interface of fresh and marine waters: flow regime changes, biogeochemical cascades and picocyanobacterial blooms—the example of Florida Bay, USA. *Biogeochemistry*. doi: 10.1007/s10533-021-00760-4.
- Glibert, P. M., Wilkerson, F. P., Dugdale, R. C., Raven, J. A., Dupont, C. L., Leavitt, P. R., et al. (2016). Pluses and minuses of ammonium and nitrate uptake and assimilation by phytoplankton and implications for productivity and community composition, with emphasis on nitrogen-enriched conditions. *Limnology and Oceanography* 61, 165–197. doi: 10.1002/lno.10203.
- Harrison, P. J., Waters, R. E., and Taylor, F. J. R. (1980). A broad spectrum artificial sea water medium for coastal and open ocean phytoplankton. *J Phycol* 16, 28–35. doi: 10.1111/j.1529-8817.1980.tb00724.x.

- Hobbie, S., Baker, L., Buyarski, C., Nidzgorski, D., and Finlay, J. (2013). Decomposition of tree leaf litter on pavement: Implications for urban water quality. *Urban Ecosystems* 17, 369–385. doi: 10.1007/s11252-013-0329-9.
- Hobbie, S. E., Finlay, J. C., Janke, B. D., Nidzgorski, D. A., Millet, D. B., and Baker, L. A. (2017). Contrasting nitrogen and phosphorus budgets in urban watersheds and implications for managing urban water pollution. *Proc Natl Acad Sci U S A* 114, 4177–4182. doi: 10.1073/pnas.1618536114.
- Huber, P., Diovisalvi, N., Ferraro, M., Metz, S., Lagomarsino, L., Llames, M. E., et al. (2017). Phenotypic plasticity in freshwater picocyanobacteria. *Environmental Microbiology* 19, 1120–1133. doi: 10.1111/1462-2920.13638.
- Hutchinson, G. E. (1957). Concluding Remarks. *Cold Spring Harb Symp Quant Biol* 22, 415–427. doi: 10.1101/SQB.1957.022.01.039.
- Jasser, I., and Callieri, C. (2016). “Picocyanobacteria,” in *Handbook of Cyanobacterial Monitoring and Cyanotoxin Analysis* (John Wiley & Sons, Ltd), 19–27. doi: 10.1002/9781119068761.ch3.
- Jezberová, J., and Komárková, J. (2007). Morphological transformation in a freshwater *Cyanobium* sp. induced by grazers. *Environmental Microbiology* 9, 1858–1862. doi: 10.1111/j.1462-2920.2007.01311.x.
- Jónasdóttir, S. H. (2019). Fatty Acid Profiles and Production in Marine Phytoplankton. *Mar Drugs* 17, E151. doi: 10.3390/md17030151.
- Kaushal, S. S., Groffman, P. M., Band, L. E., Elliott, E. M., Shields, C. A., and Kendall, C. (2011). Tracking Nonpoint Source Nitrogen Pollution in Human-Impacted Watersheds. *Environ. Sci. Technol.* 45, 8225–8232. doi: 10.1021/es200779e.
- Kay, M., Elkin, L. A., Higgins, J. J., and Wobbrock, J. O. (2021). *ARTool: Aligned Rank Transform*. Available at: <https://CRAN.R-project.org/package=ARTool> [Accessed April 11, 2022].
- Kim, Y., Jeon, J., Kwak, M. S., Kim, G. H., Koh, I., and Rho, M. (2018). Photosynthetic functions of *Synechococcus* in the ocean microbiomes of diverse salinity and seasons. *PLOS ONE* 13, e0190266. doi: 10.1371/journal.pone.0190266.
- Kjørboe, T. (2018). *A Mechanistic Approach to Plankton Ecology*. Princeton University Press doi: 10.1515/9780691190310.
- Komárek, J. (2010). Recent changes (2008) in cyanobacteria taxonomy based on a combination of molecular background with phenotype and ecological consequences (genus and species concept). *Hydrobiologia* 639, 245–259. doi: 10.1007/s10750-009-0031-3.

- Kromkamp, J. (1987). Formation and functional significance of storage products in cyanobacteria. *New Zealand Journal of Marine and Freshwater Research* 21, 457–465. doi: 10.1080/00288330.1987.9516241.
- Lenth, R. V., Buerkner, P., Herve, M., Love, J., Riebl, H., and Singmann, H. (2021). *emmeans: Estimated Marginal Means, aka Least-Squares Means*. Available at: <https://CRAN.R-project.org/package=emmeans> [Accessed April 13, 2021].
- Lindell, D., Penno, S., Al-Qutob, M., David, E., Rivlin, T., Lazar, B., et al. (2005). Expression of the nitrogen stress response gene *ntcA* reveals nitrogen-sufficient *Synechococcus* populations in the oligotrophic northern Red Sea. *Limnology and Oceanography* 50, 1932–1944. doi: 10.4319/lo.2005.50.6.1932.
- Lionard, M., Muylaert, K., Gansbeke, D. V., and Vyverman, W. (2005). Influence of changes in salinity and light intensity on growth of phytoplankton communities from the Schelde river and estuary (Belgium/The Netherlands). *Hydrobiologia* 540, 105–115. doi: 10.1007/s10750-004-7123-x.
- Liu, Y., Villalba, G., Ayres, R. U., and Schroder, H. (2008). Global Phosphorus Flows and Environmental Impacts from a Consumption Perspective. *Journal of Industrial Ecology* 12, 229–247. doi: 10.1111/j.1530-9290.2008.00025.x.
- Lopes, V. R., Ramos, V., Martins, A., Sousa, M., Welker, M., Antunes, A., et al. (2012). Phylogenetic, chemical and morphological diversity of cyanobacteria from Portuguese temperate estuaries. *Marine Environmental Research* 73, 7–16. doi: 10.1016/j.marenvres.2011.10.005.
- MacCormack, A. (2021). High-throughput analysis of picocyanobacterial growth responses to a matrix of conditions.
- Malerba, M. E., Palacios, M. M., Palacios Delgado, Y. M., Beardall, J., and Marshall, D. J. (2018). Cell size, photosynthesis and the package effect: an artificial selection approach. *New Phytologist* 219, 449–461. doi: 10.1111/nph.15163.
- Mangiafico, S. (2016). *Summary and Analysis of Extension Program Evaluation in R*. 1.19.10. Available at: <https://rcompanion.org/handbook/index.html> [Accessed March 28, 2022].
- Mueller, C., Zink, M., Samaniego, L., Krieg, R., Merz, R., Rode, M., et al. (2016). Discharge Driven Nitrogen Dynamics in a Mesoscale River Basin As Constrained by Stable Isotope Patterns. *Environ Sci Technol* 50, 9187–9196. doi: 10.1021/acs.est.6b01057.
- Oksanen, J., Blanchet, F. G., Friendly, M., Kindt, R., Legendre, P., McGlenn, D., et al. (2020). *vegan: Community Ecology Package*. Available at: <https://CRAN.R-project.org/package=vegan> [Accessed April 11, 2022].

- Palenik, B., Brahamsha, B., Larimer, F. W., Land, M., Hauser, L., Chain, P., et al. (2003). The genome of a motile marine *Synechococcus*. *Nature* 424, 1037–1042. doi: 10.1038/nature01943.
- Pyhälä, M., Fleming-Lehtinen, V., Laamanen, M., Łysiak-Pastuszek, E., Carstens, M., Leppänen, J.-M., et al. (2014). “Eutrophication status of the Baltic Sea 2007-2011 – A concise thematic assessment,” in *Baltic Sea Environment Proceedings* (Helsinki, Finland: HELCOM).
- Raven, J. A. (1998). The twelfth Tansley Lecture. Small is beautiful: the picophytoplankton. *Functional Ecology* 12, 503–513. doi: 10.1046/j.1365-2435.1998.00233.x.
- Redfield, A. C. (1934). On the proportions of organic derivatives in sea water and their relation to the composition of plankton. *The University Press James Johnstone Memorial Volume*, 176–192.
- Ruess, L., and Müller-Navarra, D. C. (2019). Essential Biomolecules in Food Webs. *Frontiers in Ecology and Evolution* 7. Available at: <https://www.frontiersin.org/article/10.3389/fevo.2019.00269> [Accessed March 28, 2022].
- Schindler, D. W. (2006). Recent advances in the understanding and management of eutrophication. *Limnology and Oceanography* 51, 356–363. doi: 10.4319/lo.2006.51.1_part_2.0356.
- Schmidt, K., Birchill, A. J., Atkinson, A., Brewin, R. J. W., Clark, J. R., Hickman, A. E., et al. (2020). Increasing picocyanobacteria success in shelf waters contributes to long-term food web degradation. *Global Change Biology* 26, 5574–5587. doi: 10.1111/gcb.15161.
- Shangguan, Y., Glibert, P. M., Alexander, J., Madden, C. J., and Murasko, S. (2017). Phytoplankton assemblage response to changing nutrients in Florida Bay: Results of mesocosm studies. *Journal of Experimental Marine Biology and Ecology* 494, 38–53. doi: 10.1016/j.jembe.2017.05.006.
- Stal, L. J., Albertano, P., Bergman, B., Bröckel, K. von, Gallon, J. R., Hayes, P. K., et al. (2003). BASIC: Baltic Sea cyanobacteria. An investigation of the structure and dynamics of water blooms of cyanobacteria in the Baltic Sea—responses to a changing environment. *Continental Shelf Research* 23, 1695–1714. doi: 10.1016/j.csr.2003.06.001.
- Stockner, J. G. (1988). Phototrophic picoplankton: An overview from marine and freshwater ecosystems. *Limnology and Oceanography* 33, 765–775. doi: 10.4319/lo.1988.33.4part2.0765.
- Thompson, A. W., van den Engh, G., Ahlgren, N. A., Kouba, K., Ward, S., Wilson, S. T., et al. (2018). Dynamics of *Prochlorococcus* Diversity and Photoacclimation

During Short-Term Shifts in Water Column Stratification at Station ALOHA. *Frontiers in Marine Science* 5. Available at: <https://www.frontiersin.org/article/10.3389/fmars.2018.00488> [Accessed March 28, 2022].

- Tilman, D. (1999). Global environmental impacts of agricultural expansion: The need for sustainable and efficient practices. *Proceedings of the National Academy of Sciences* 96, 5995–6000. doi: 10.1073/pnas.96.11.5995.
- Watanabe, M. M., Kawachi, M., Hiroki, M., and Kasai, F. (2000). *NIES Collection List of Strains. Sixth Edition, 2000, Microalgae and Protozoa*. Sixth Edition. Tsukuba, Japan: National Institute for Environmental Studies.
- Wickham, H., Averick, M., Bryan, J., Chang, W., McGowan, L. D., François, R., et al. (2019). Welcome to the Tidyverse. *Journal of Open Source Software* 4, 1686. doi: 10.21105/joss.01686.
- Wu, Y., Campbell, D. A., Irwin, A. J., Suggett, D. J., and Finkel, Z. V. (2014). Ocean acidification enhances the growth rate of larger diatoms. *Limnology and Oceanography* 59, 1027–1034. doi: 10.4319/lo.2014.59.3.1027.
- Xu, H., Paerl, H. W., Qin, B., Zhu, G., and Gao, G. (2010). Nitrogen and phosphorus inputs control phytoplankton growth in eutrophic Lake Taihu, China. *Limnology and Oceanography* 55, 420–432. doi: 10.4319/lo.2010.55.1.0420.
- Yan, P., Guo, J., Zhang, P., Xiao, Y., Li, Z., Zhang, S., et al. (2021). The role of morphological changes in algae adaptation to nutrient stress at the single-cell level. *Science of The Total Environment* 754, 142076. doi: 10.1016/j.scitotenv.2020.142076.
- Yang, Y.-Y., and Lusk, M. G. (2018). Nutrients in Urban Stormwater Runoff: Current State of the Science and Potential Mitigation Options. *Curr Pollution Rep* 4, 112–127. doi: 10.1007/s40726-018-0087-7.
- Yi, Q., Chen, Q., Hu, L., and Shi, W. (2017). Tracking Nitrogen Sources, Transformation, and Transport at a Basin Scale with Complex Plain River Networks. *Environ. Sci. Technol.* 51, 5396–5403. doi: 10.1021/acs.est.6b06278.
- Zavřel, T., Faizi, M., Loureiro, C., Poschmann, G., Stühler, K., Sinetova, M., et al. (2018). Quantitative insights into the cyanobacterial cell economy. 446179. doi: 10.1101/446179.
- Zorz, J. (2019). Analyzing Microbial Ecology Data in R. Available at: <https://jkzorz.github.io/> [Accessed March 28, 2022].

Appendix

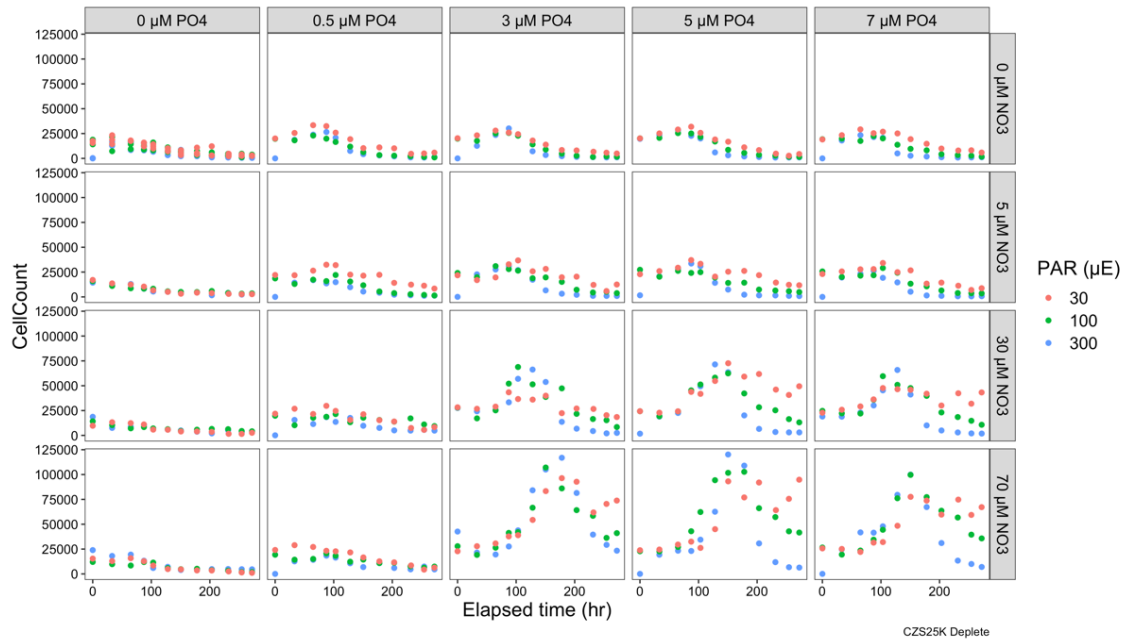


Figure 1: CZS25K cell counts collected using a cytometer. Cell count changes are represented against elapsed growth time with hour as the time unit. Culture conditions are faceted by nitrate and phosphate concentrations (μM), and point colour is used to represent variation in light intensity.

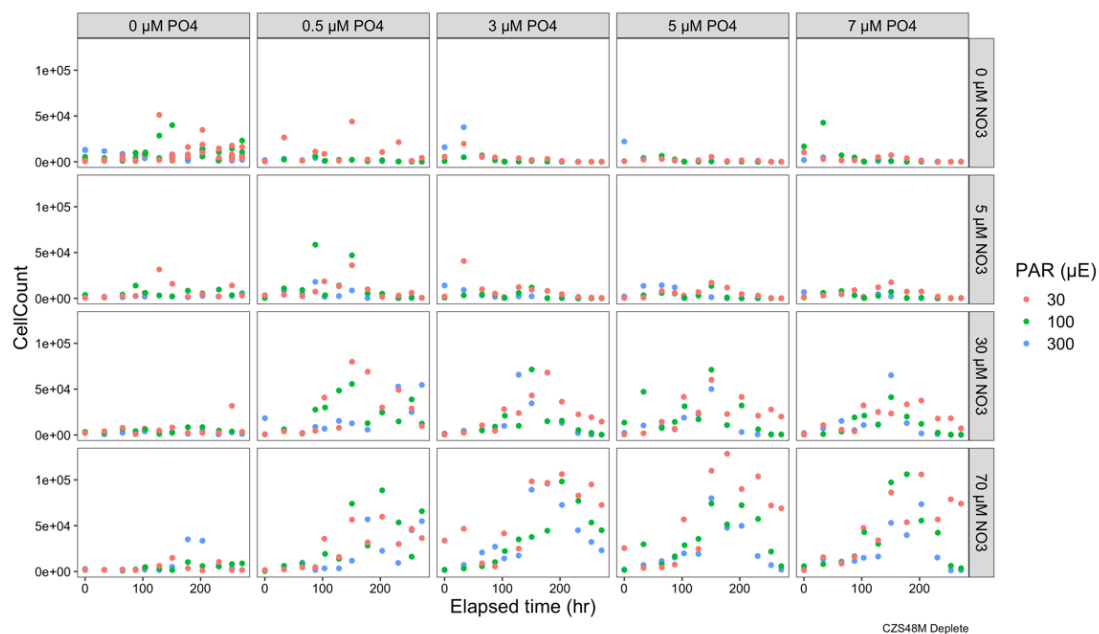


Figure 2: CZS48M cell counts collected using a cytometer. Cell count changes are represented against elapsed growth time with hour as the time unit. Culture conditions are faceted by nitrate and phosphate concentrations (μM), and point colour is used to represent variation in light intensity.

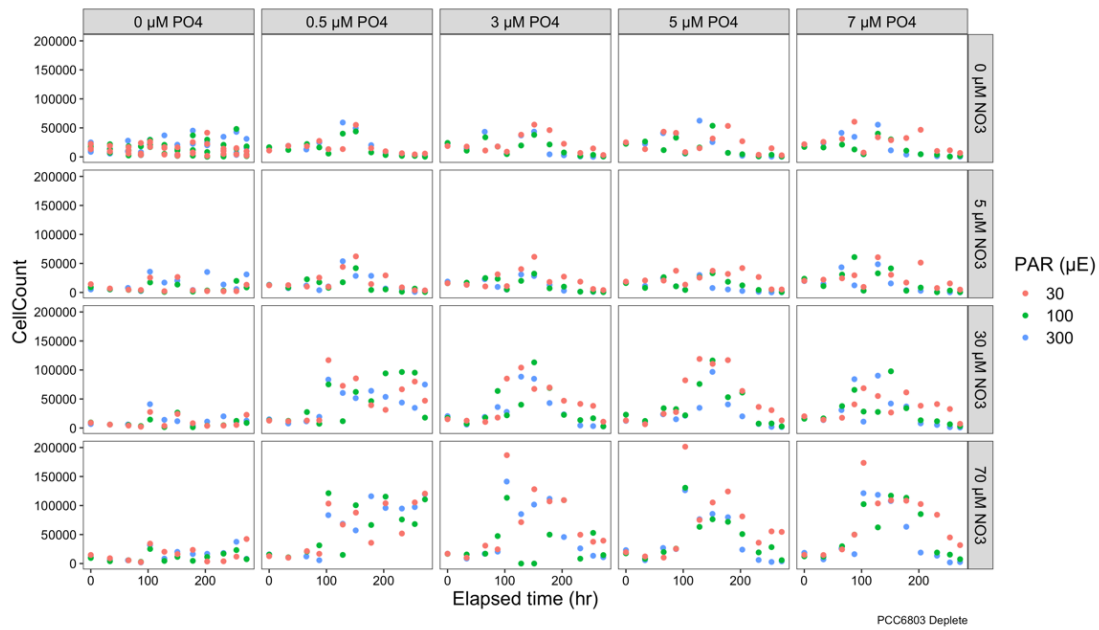


Figure 3: PCC6803 cell counts collected using a cytometer. Cell count changes are represented against elapsed growth time with hour as the time unit. Culture conditions are faceted by nitrate and phosphate concentrations (μM), and point colour is used to represent variation in light intensity.